# Damage localization based on vibrations

Benjamin Fasquelle, Nicolas Pompidor and Jimmy Rogala

**Abstract**

***Index Terms*—Damage, Localization, Vibration, Health monitoring**

## I. Introduction

The process of implementing a damage identification strategy for aerospace, civil and mechanical engineering infrastructure is referred as a structural health monitoring (SHM) [5].

In the most general terms, damage can be defined as changes in a system that negatively affect its current or future performance. In general, a damage can be observed by comparing two different states of the system, one of which is supposed to represent the initial often undamaged state.

Almost all industries want to detect damage in their infrastructure as quickly as possible whether for the potential life-safety or economic impact. Such detection requires these industries to perform some form of SHM.

Clearly, such damage identification has significant life-safety implications. For instance, there are no quantifiable methods to determine if buildings should be repaired after an earthquake yet. SHM may one day provide the technology that can be used to significantly minimize the uncertainty associated with such post-earthquake damage assessments. Thus additional catastrophes could be avoided.

Generally, the damage identification can be divided into four levels [10]:

- detection: Is the structure damaged or not?
- localization: Where is the damaged area located?
- quantification: What is the extent of damage?
- prediction: What is the remaining service life of the structure?

Traditional methods of damage detection based on visual inspections or experimental techniques such as radiography or ultrasound allow to obtain detailed information about a local damage state but requires to know area where it is located (and hope for easy access). These techniques may be costly, taking a long time to be performed and impractical to detect damage in large urban areas. Furthermore, they may fail if damage is not visibly evident. This is why other global methods automated and based on sensor measurements were developed.

The purpose of this work is the analysis of a particular data-driven damage localization method, namely the FRF interpolation method [3], and the development of a statistical extension of this method. This paper is organized as follows. In section II we present the existing methods (model-based and data driven methods), then in section III we detail the different models of vibrating structures and finally, in section IV we talk about the localization using FRF interpolation method and, finally, its results in section V.

## II. State of the art

The use of methods based on recorded responses proved to perform as valuable alternatives. The general idea for vibration-based damage identification is that the damage affects the physical properties (mass, damping, and stiffness) of the structure, and this will cause detectable changes in modal properties (natural frequencies, modal damping, and mode shapes). For instance, cracks cause reductions in stiffness. Therefore, by analyzing the physical properties of the structure a damage can be detected.

Most of the different vibration based damage identification methods can be classified as data-driven or model-based. The model-based methods assume that a detailed numerical model of the structure is available for damage identification and, by vibration measurements, updates the model parameters. On another side, data-driven methods are based solely on the recorded response. These methods are interesting for a real-time damage identification but unavailability of a numerical model often hinders the estimation of damage severity. A third group includes data-driven methods that use finite element (FE) information without model updating.

### A. Model-based methods

In model-based methods, damage is identified through the updating of a finite element (FE) model. Most of the time, modal characteristics is the experimental data used for damage assessment through FE model updating.Different types of modal data can be used. For changes in structural stiffness, model updating can be performed based only on natural frequencies or eigenvalues which are known to change in this case. Detailed informations about model-based methods can be found in references [8], [13] and [11].

### B. Data driven methods

Data driven methods are inverse methods that use models based on experimental response data recorded on the structure instead of physical models [9]. In these methods, the damage parameter $D$ is the variation of the damage feature $d$ between the inspection $I$ and the reference $R$ configurations:

$$D = d_I - d_R \tag{1}$$

Data-driven methods do not require a FE model and may be applied with a limited number of available signals (both responses and excitations). To extract the damage features, different signal-processing tools can be used. Therefore, depending on the tool, data-driven methods can be classified in Fourier-based methods, Time series method and Time-variant methods. A more detailed description of these methods can be

found in references [6] and [12]. The analyzed method in this paper belongs to this class.

### C. Combined data-driven and model-based methods

A third group of methods for damage localization and quantification lies between the data-driven and model-based approaches. "This class is based on datadriven features from measurements of the reference and damaged states, which are confronted to a FE model of the structure to define damage indicators for the elements of the FE model, without updating its parameters" [9].

## III. Models of vibrating structures

### A. Finite element model

The dynamic behaviour of a mechanical system consisting of $n$ degrees of freedom (see Figure (1)) is described by following matrix differential equation:

$$M\ddot{q}(t) + C\dot{q}(t) + Kq(t) = f(t) \tag{2}$$

where $q(t)$ is the displacement vector at a continous time $t$, and $M, C, K \in \mathbb{R}^{n\times n}$, are the mass, damping and stiffness matrices.

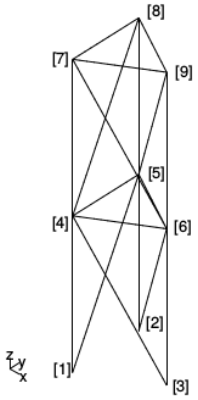


Fig. 1. Finite element model, from [10]

For civil engineering structures, Equation (2) is obtained as the finite element approximation of the system with only $n$ dregrees of freedom. The structure is divided in elements, and the global mass matrix $M$ and stiffness matrix $K$ are generated from the geometry and material properties of the elements.

### B. Continous-time state-space model

From the Equation (2) and with the variable change $x = \begin{pmatrix}\dot{q}\\ q\end{pmatrix}$, we obtain the state equation:

$$\dot{x}(t) = A_c x(t) + B_c f(t) \tag{3}$$

where $A_c = \begin{pmatrix}0 & I\\ M^{-1}K & M^{-1}C\end{pmatrix}$ and $B_c = \begin{pmatrix}0\\ M^{-1}\end{pmatrix}$

In a practical vibration experiment, not all $n$ degrees of freedom of the structure are measured, but only a subset. The observation equation is:

$$y(t) = C_c x(t) + D_c f(t) \tag{4}$$

If it is assumed that all $n$ degrees of freedom are measured and that the sensors are accelerometers transducers, we have $C_c = \begin{pmatrix}M^{-1}K & M^{-1}C\end{pmatrix}$ and $D_c = \begin{pmatrix}M^{-1}\end{pmatrix}$

Thus, the classical continuous-time state-space model is:

$$\begin{cases}\dot{x}(t) = A_c x(t) + B_c f(t)\\ y(t) = C_c x(t) + D_c f(t)\end{cases} \tag{5}$$

### C. Discrete-time state-space model

Up to now all equations were expressed in continuous time, whereas in reality measurements are taken at discrete time instants. So this model need to be converted to discrete time. Another reason is that it is needed for performing simulations.

Thus, we choose a certain fixed sampling period $\Delta t$, and the continuous-time equations are discretized and solved at all discrete time instants $k$ with $t = k\Delta t, k \in \mathbb{N}$.

The discrete-time state-space model is:

$$\begin{cases}x_{k+1} &= A_d x_k + B_d f_k\\ y_k &= C_d x_k + B_d f_k\end{cases} \tag{6}$$

where

$$\begin{aligned}A_d &= exp(A_c \Delta t)\\ B_d &= (A_d - I)A_c^{-1}B_c\\ C_d &= C_c\\ D_d &= D_c\end{aligned} \tag{7}$$

## IV. Localization using FRF interpolation method

This method is presented in [3]. The main hypothesis underlying the method is that a concentrated damage reflects in a loss of spatial regularity of the vibrational profile of a structure, compared with the reference (undamaged) state.

In this section, we suppose that we have $n$ sensors, which are located along an axis $z$, and we denote them by $\{z_l\}, l \in \{1...n\}$. We also suppose we have $N$ measurements for each sensor.

For each sensor, we calculate the Frequency Response Function (FRF) from the acceleration's measures, at certain frequencies (which are $\frac{k}{N}, k \in \{0...N-1\}$).

Thus, for each frequency and each sensor, we have the transfer function value. Let us denote $H_R(z_l, f_i)$ the value of the transfer function for the sensor $z_l$ at the frequency $f_i$.

Then, we calculate for each sensor $z_l$ the cubic polynomial spline interpolation of the transfer functions $H_R(z_k, f_i)$ measured at all the other instrumented locations $\{z_k\}, k \in \{1...n\}, k \neq l$: we denote it $H_S(z_l, f_i)$.

For these two transfer functions, we define the interpolation error $E(z_l, f_i)$ as the absolute value of the difference between recorded and interpolated FRFs:

$$E(z_l, f_i) = |H_R(z_l, f_i) - H_S(z_l, f_i)| \tag{8}$$

Since we want to characterize each location $z_l$ with a scalar-valued error index, we introduce the norm of the error on the whole range of frequencies:

$$E(z_l) = \sqrt{\sum_{i=1}^{N} E^2(z_l, f_i)} \tag{9}$$

Transfer function values obviously depend on the state of the structure. Hence, if the estimation of the error function

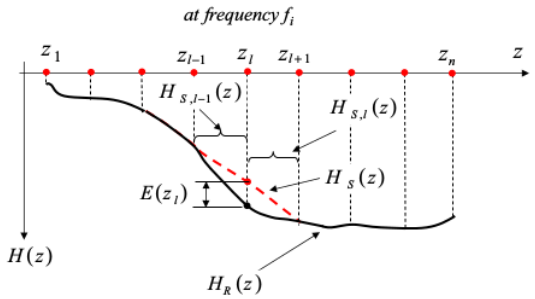


Fig. 2. Interpolation error, from [3]

through Equation (9) is repeated in the baseline (undamaged) and in the inspection (possibly damaged) configuration, then the difference between the two values, denoted respectively by $E_0(z_l)$ and $E_d(z_l)$, can provide an indication about the existence of degradation at location $z_l$:

$$\Delta E(z_l) = E_d(z_l) - E_0(z_l) \tag{10}$$

An increase in the interpolation error between the reference configuration and the current configuration at a station $z_l$ , i.e. $\Delta E(z_l) > 0$, highlights a localized reduction of smoothness in the vibrational amplitude profile and, therefore, it is assumed to be a symptom of a local variation of stiffness at $z_l$ associated with the occurrence of damage.

The above analysis has been developed in a deterministic context. Several sources, such as temperature, nonlinear behavior, soil structure interaction and noise in recorded data, can induce variations of the interpolation error even if no damage occurs.

Thus, once have to determine a threshold $E_T$, such as $\Delta E(z_l)$ must be taller than $E_T$ to have a high probability of identification of a damage at location $z_l$. Indeed, as we can see in the Figure (3), the curves which represent the fact to have a damage or not have a share area: if the interpolation error $\Delta E(z_l)$ is in this area, one can commit two errors:

- if it is in the area $P_f(z_l)$ under the graph of $p_{E,0}(z_l)$, once can detect a damage since there isn't one (false alarm).
- if it is in the area $P_m(z_l)$ under the graph of $p_{E,d}(z_l)$, once can not detect a damage since there is one (missing alarm).

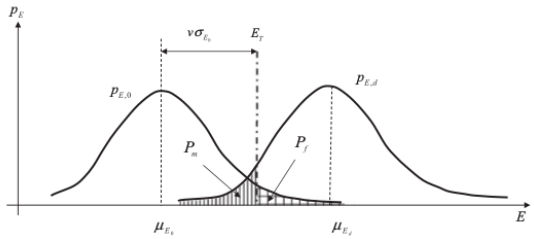


Fig. 3. Probabilities of false and missing alarm, from [3]

A detailled analysis of the statistical behaviour of the interpolation error is envisaged in the second part of this project.

## V. Simulation

### A. Obtaining acceleration measures

We have implemented a simulation to check this method of localization. We made this on the following system: $n$ masses, connected through springs and dampers. We denote the masses $\{m_i\}_{i=1}^n$, the springs stifness $\{k_i\}_{i=1}^n$ and the dampers $\{c_i\}_{i=1}^n$ (see Figure (4)).

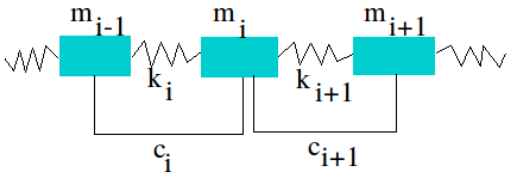


Fig. 4. Masses connected through springs and dampers

For the simulation, we use the discrete-time state-space model (Equation (6)). First, we needed the matrices $M, C, K$. In this case, the matrices $M$ and $K$ are given by:

$$M = \begin{pmatrix} m_1 & & \\ & \ddots & \\ & & m_n \end{pmatrix}$$
$$K = \begin{pmatrix} k_1 + k_2 & -k_1 & & & & \\ -k_1 & \ddots & & & & \\ & -k_i & k_i + k_{i+1} & -k_{i+1} & & \\ & & & \ddots & -k_n & \\ & & & -k_n & k_n & \end{pmatrix} \tag{11}$$

Due to the lack of identifiable or measurable material constants that govern the global damping behaviour of a structure, it is generally impossible to assemble the damping matrix C in the same way as M and K. Thus, we do the same thing that in practical situations: we consider that we are in the case of Rayleigh, i.e. a linear combination of the mass and stiffness matrix:

$$C = \alpha M + \beta K, \qquad \alpha, \beta \in \mathbb{R}_+ \tag{12}$$

With this matrices, we can calculate the matrices $A_c, B_c, C_c$ and $D_c$. To calculate the matrices $A, B$, we have to know the sampling period $\Delta t$. We need the frequencies of the system, because we have to respect the NyquistShannon sampling theorem. To determine the Nyquist frequency (here, it is the taller frequency of the system), we calculate the eigenvalues of $A_c$. Indeed, we have the link between the eigenvalues $\{\lambda_i\}_{i=1}^n$ and the frequencies of the system $\{f_i\}_{i=1}^n$:

$$\lambda_i = -\omega_i \xi_i \pm i\omega_i \sqrt{1 - \xi_i^2} \tag{13}$$

where $\omega_i = 2\pi f_i$ and $\xi_i$ is the damping ratio.

**Remark 1.** *We can see that:*
$|\lambda_i| = \sqrt{\omega_i^2 \xi_i^2 + \omega_i^2 (1 - \xi_i^2)} = \omega_i$

**Remark 2.** *The matrix $A_c$ has $2 \times n$ eigenvalues, but we obtain $n$ frequencies (for each eigenvalues, another one is its conjugated complex).*

Now, we have the sampling period:

$$\Delta t = 2 \times max_{i \in \{1...n\}} f_i \tag{14}$$

So we can calculate the matrices $A, B$ and make the simulation with the discrete-time state-space model (Equation (6)). To simulate the forces $f_k$, we use a white noise.

### B. Frequency Response Function

The FRF correspond to the transfer function of the system. In frequency domain, if $F$ is the force that is apply on the system and $S$ is the response of this force, the FRF is given by:

$$H = \frac{S}{F} \tag{15}$$

We want to calculate the FRF of the system, for each sensor localization. Here, we calculate an estimation of the FRF, called $H_1$ estimator [2]. We suppose we have a vector of the forces $\{f_k\}_{k=1}^N$ and a vector of the accelerations $\{y_k\}_{k=1}^N$ for each sensor (the two vectors are size $N$). We need to be in frequency domain, so we calculate the discrete Fourier transform:

$$\begin{aligned} F_n &= \sum_{k=1}^{N} f_k e^{-2i\pi kn/N} \qquad n \in \{1...N\} \\ Y_n &= \sum_{k=1}^{N} y_k e^{-2i\pi kn/N} \qquad n \in \{1...N\} \end{aligned} \tag{16}$$

Then we calculate the power spectra, i.e. the Auto Power spectra of the inputs and the outputs and the Cross Power spectra between the inputs and outputs respectively given by:

$$\begin{aligned} S_{ff}(n) &= F_n F_n^H \qquad n \in \{1...N\} \\ S_{yf}(n) &= Y_n F_n^H \qquad n \in \{1...N\} \end{aligned} \tag{17}$$

where $M^H$ is the Hermitian of the matrix $M$. Thus, the FRF is given by:

$$H_1(n) = S_{yf}(n) S_{ff}(n)^{-1} \tag{18}$$

**Remark 3.** *If we consider each sensor separately, $F_n$ and $Y_n$ are scalars, so we have:*

$$\begin{aligned} H_1(n) &= S_{yf}(n) S_{ff}(n)^{-1} \\ &= Y_n F_n^H (F_n F_n^H)^{-1} \\ &= Y_n / F_n \end{aligned} \tag{19}$$

### C. Interpolation

We have to calculate for each sensor $z_l$ and for each considered frequency $f_i$ the cubic polynomial spline interpolation of the transfer function $H_R(z_k, f_i)$. The cubic spline interpolation is a piecewise continuous curve, passing through each of the values. There is a separate cubic polynomial interpolation for each interval, each with its own coefficients. Cubic polynomial spline interpolations produce an interpolated function that is continuous through to the second derivative.

With this interpolation, we can calculate the error as it is described in the section IV.

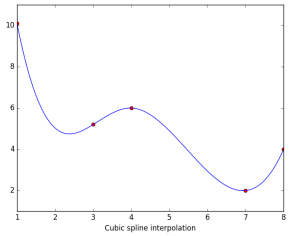


Fig. 5. Cubic spline interpolation

### D. Results

For the following simulation results, we consider a system with 10 masses. We put a sensor on each mass. For the damaged state, we lower the stifness of the spring between sensors 4 and 5 by 90%. The values of the FRF on the figures are the norm of the FRF values.

Figure (6) presents results of the FRF on the simulation datas: here is the curve of the FRF of one sensor, against frequencies. We can see three peaks which are at the natural frequencies of the system, but there is one of these frequencies which not present a peak. Seeing this curve for each sensor, we observed that certain sensors have one peak for each natural frequencies, and others sensors have one peak for each except one, relied on the position of the sensor in the system. It is problematic because it is around the natural frequencies of the system that we have better datas, but if certain sensors haven't response with certain frequencies, we could miss out on a damage.

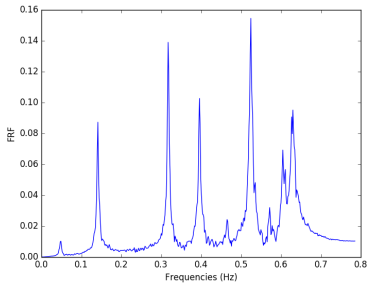


Fig. 6. FRF of one sensor (ten in total), against frequencies

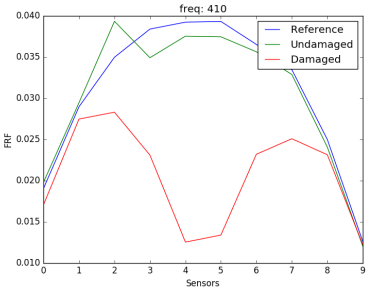


Fig. 7. FRF values for 10 sensors, at a fixed frequency (damage between sensors 4 and 5

Figure (7) is the FRF values for the ten sensors (at a fixed frequency). Here, we easily can see that there is a damage between the sensors 4 and 5 (as we noticed it). However, as the damaged FRF is away from the reference FRF, we can see that there isn't a significant loss of regularity at sensors 4 and 5 (the interpolation error isn't high).

Figure (8) is the FRF values for the same ten sensors that in Figure (7), with the same damage, at a different frequency. Here, we can see a significant loss of regularity at sensors 6 and 8. It shows that we have to select the frequencies where we calculate the interpolation error. Indeed, an hypothesis is that significant values of the FRF are near to the natural frequencies of the system (that we can see in Figure (6)).

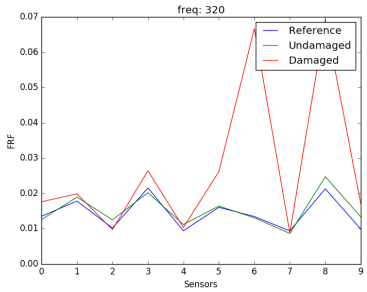


Fig. 8. FRF values for 10 sensors, at a fixed frequency (damage between sensors 4 and 5

Finaly, we can see in Figure (9) the global error described in section IV. The two first and last values (i.e. for sensor 0,1,8 and 9) aren't useful because cubic spline interpolation requires two values on each side of the interpolate value. We can see that, if we consider all frequencies for the error calcul, results aren't as we want: here the damaged system has a FRF more regular than the undamaged system. A selection of the frequencies is necessary.

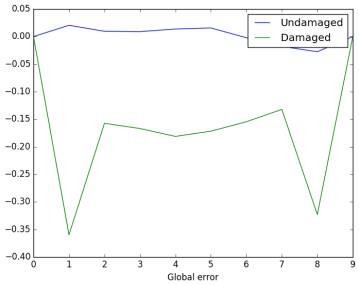


Fig. 9. FRF values for 10 sensors, at a fixed frequency (damage between sensors 4 and 5

## VI. Conclusion

In this paper, we presented the structure heatlh monitoring and a state of the art for this. Then we detailled one of the methods, the FRF interpolation method, and some physical models. Last, we presented our simulation with a sping-mass system and our results with the implementation of the FRF interpolation method.

We saw that we have to do a selection of the frequencies where we calculate the interpolation error.

In the second part of this project, we will do a detailled analysis of the statistical behaviour of the interpolation error.

## References

[1] James MW Brownjohn. "Structural health monitoring of civil infrastructure". In: *Philosophical Transactions of the Royal Society of London A: Mathematical, Physical and Engineering Sciences* 365.1851 (2007), pp. 589–622.

[2] Bart Cauberghe. "Applied frequency-domain system identification in the field of experimental and operational modal analysis". In: *Praca doktorska, VUB, Brussel* (2004).

[3] M Dilena, MP Limongelli, and A Morassi. "Damage localization in bridges via the FRF interpolation method". In: *Mechanical Systems and Signal Processing* 52 (2015), pp. 162–180.

[4] Wei Fan and Pizhong Qiao. "Vibration-based damage identification methods: a review and comparative study". In: *Structural Health Monitoring* 10.1 (2011), pp. 83–111.

[5] Charles R Farrar and Keith Worden. "An introduction to structural health monitoring". In: *Philosophical Transactions of the Royal Society of London A: Mathematical, Physical and Engineering Sciences* 365.1851 (2007), pp. 303–315.

[6] Spilios D Fassois and John S Sakellariou. "Time-series methods for fault detection and identification in vibrating structures". In: *Philosophical Transactions of the Royal Society of London A: Mathematical, Physical and Engineering Sciences* 365.1851 (2007), pp. 411–448.

[7] Michael I Friswell. "Damage identification using inverse methods". In: *Philosophical Transactions of the Royal Society of London A: Mathematical, Physical and Engineering Sciences* 365.1851 (2007), pp. 393–410.

[8] C-P Fritzen, D Jennewein, and Th Kiefer. "Damage detection based on model updating methods". In: *Mechanical systems and signal processing* 12.1 (1998), pp. 163–186.

[9] M Limongelli et al. "Towards extraction of vibration-based damage indicators". In: *Proceedings of the 8th European Workshop On Structural Health Monitoring (EWSHM 2016)*. 2016.

[10] Bart Peeters. "System identification and damage detection in civil engineering". In: *Department of Civil Engineering, Katholieke Universiteit Leuven, Leuven* (2000), p. 233.

[11] Ellen Simoen, Guido De Roeck, and Geert Lombaert. "Dealing with uncertainty in model updating for damage assessment: A review". In: *Mechanical Systems and Signal Processing* 56 (2015), pp. 123–149.

[12] Wiesław J Staszewski and Amy N Robertson. "Time–frequency and time–scale analyses for structural health monitoring". In: *Philosophical Transactions of the Royal Society of London A: Mathematical, Physical and Engineering Sciences* 365.1851 (2007), pp. 449–477.

[13] Anne Teughels and Guido De Roeck. “Damage detection and parameter identification by finite element model updating”. In: *Revue européenne de génie civil* 9.1-2 (2005), pp. 109–158.